

Electrochemical investigation of Li–Al anodes in oligo(ethylene glycol) dimethyl ether/LiPF₆

Y. N. Zhou · X. J. Wang · H. S. Lee ·
K. W. Nam · X. Q. Yang · O. Haas

Received: 2 January 2010 / Accepted: 15 October 2010 / Published online: 10 November 2010
© U.S. Government 2010

Abstract 1 M LiPF₆ dissolved in oligo(ethylene glycol) dimethyl ether with a molecular weight 500 g mol⁻¹ was investigated as a new electrolyte (OEGDME500, 1 M LiPF₆) for metal deposition and battery applications. At 25 °C a conductivity of 0.48×10^{-3} S cm⁻¹ was obtained and at 85 °C, 3.78×10^{-3} S cm⁻¹. The apparent activation barrier for ionic transport was evaluated to be 30.7 kJ mol⁻¹. OEGDME500, 1 M LiPF₆ allows operating temperature above 100 °C with very attractive conductivity. The electrolyte shows excellent performance at negative and positive potentials. With this investigation, we report experimental results obtained with aluminum electrodes using this electrolyte. At low current densities lithium ion reduction and re-oxidation can be achieved on aluminum electrodes at potentials about 280 mV more positive than on lithium electrodes. In situ X-ray diffraction measurements collected during electrochemical lithium deposition on aluminum electrodes show that the shift to positive potentials is due to the negative Gibbs free energy change of the Li–Al alloy formation reaction.

Keywords Electrolytes · Electrochemical stability · Conductivity · Oligo(ethylene glycol) dimethyl ether · Li–Al alloy formation

1 Introduction

For lithium battery applications, it would be advantageous to have electrolyte solvents with higher boiling points than the presently most popular carbonate solvents. Ethylene carbonates and propylene carbonates are not stable enough at highly reactive lithium electrodes and could develop too much pressure at high power batteries [1, 2]. Solid polymer electrolytes based on poly(ethylene glycol) have been investigated extensively [3–7], but the ionic conductivity of these electrolytes is not high enough for high power applications [5–7]. The conductivity can be increased if low molecular weight oligo(ethylene glycols) are used as plasticizers and if strong anion complexing agents are used to reduce ion pair formation [8]. Addition of nanoparticle fillers such as Al₂O₃ or TiO₂ helps also to enhance the conductivity of these polymer electrolytes [7]. Oligo(ethylene glycols) OEG can be used as liquid electrolyte solvents with good solubility for electrolyte salts and more attractive conductivities than solid polymer electrolytes based on poly(ethylene glycol).

OEGDME or PEGDME : CH₃—O—(CH₂—CH₂—O)_n—CH₃

OEGDME are liquid solvents with high boiling points and high electrochemical stability comparable with ionic liquids but with the advantage of a lower melting point. They are therefore good candidates as aprotic electrolyte solvents for lithium battery applications and alkaline metal deposition. However, we found that the commercial available oligo(ethylene glycol) dimethyl ether MW: 250

Y. N. Zhou · X. J. Wang · H. S. Lee · K. W. Nam ·
X. Q. Yang · O. Haas
Chemistry Department, Brookhaven National Lab., Upton,
NY 11973, USA

Y. N. Zhou
Materials Science Department, Fudan University,
Shanghai 200433, China

O. Haas (✉)
Energy and Material Research Consulting,
6648 Minusio, Switzerland
e-mail: otto.haas@bluewin.ch

with $n = 3$ and $n = 4$ tend to form two separated phases if 1 M LiPF₆ is added. It is well known that OEG with 4–8 ethylene glycol units, tend to form insoluble Li⁺–PEG complexes [9, 10]. This is not the case for OEGDME500, 1 M LiPF₆, which contains [10, 11] ethylene glycol units. OEGDME500, 1 M LiPF₆ forms clear solutions with a reasonable conductivity. In addition to the safety aspect, the high boiling point of this solvent offers an unproblematic dehydration of the electrolyte. We studied this electrolyte at negative potentials investigating the reversible electrochemical Li-ion reduction and re-oxidation on Al electrodes. In an upcoming publication, we shall report investigations at positive potentials using Li_xFePO₄ electrodes to study reversible Li insertion [11].

The electrochemical behavior of aluminum electrodes and the formation of Al–Li alloys in aprotic electrolytes have been studied by several research groups. Most recently Suresh et al. [12] published a paper investigating Al electrodes in EC/DMC, 1 M LiBF₄, where they claimed that the Al–Li electrodes would be ideal dendrite free anodes for Li-battery application.

Oligo(ethylene glycols) have been used as plasticizers in polymer electrolytes as far as we know there exists no report about the electrochemical behavior of aluminum using OEGDME500, 1 M LiPF₆ as electrolyte.

2 Experimental

2.1 Electrolyte preparation

OEGDME500 was purchased from Aldrich, it was dissolved in dimethyl ether and passed through an activated carbon column. The ether was then evaporated and the residue dried in a BÜCHI Rotavapor at 60 °C and 0.3 mbar for 24 h. The product (OEGDME500) was stored under Ar in a dry box. 1.52 g LiPF₆ was added to 10 mL OEGDME500, and dissolved during about 3–4 days, while the mixture was shaken from time to time until all of the salt was completely dissolved. The solution could be stored over several weeks. However, after about 3 weeks a bluish color developed, indicating some sort of charge transfer complex formation, which, however, apparently had no remarkable influence to the electrochemical behavior of the electrolyte. For long-term application, however, it may be advantageous to use another Lithium salt. The development of a bluish color is not observed if LiBF₄ is used as an electrolyte salt.

2.2 Conductivity measurements

Conductivity measurements were performed using Hewlett-Packard 4192A impedance analyzer in a frequency

range from 1 to 1,000 kHz. A standard glass cell with two Pt electrodes was used for conductivity measurements. The cell constant was determined using a standard 0.01 M KCl aqueous solution.

2.3 Electrochemical experiments

The cyclic voltammogram was performed with a bar electrode, which was dipped into the electrolyte. The bar electrode had three electrodes embedded in epoxy resin, where at the front of the bar the three electrodes (Al electrode diameter: surface 0.05 cm², Pt electrode 0.05 cm², non-aqueous Ag/AgCl electrode 0.005 cm²) were exposed as disc electrodes. The working, counter and reference disc electrodes were arranged alongside. The Ag electrode was shortly treated with a mixture of HNO₃ and HCl to form an AgCl layer at the surface. A gas tight electrolyte vessel was loaded with the electrolyte and the bar electrode in an argon glove box then cycled outside the glove box under argon using a Solartron electrochemical equipment.

For the experiments with larger electrodes (2.8 cm²) Al foil electrodes were used in an electrochemical cell as described in a previous work [13]. High purity Al foil (thickness = 25 µm) was used as Al electrode and a Li foil (0.25 mm thick) as counter electrode, which was supported by a copper foil. The electrodes were separated by a filter paper or a Cellgard membrane, which was first soaked in with electrolyte.

2.4 In situ XRD measurements

The in situ XRD cell with Mylar windows used in these experiments has been described in detail elsewhere [14]. In situ XRD spectra were collected on beam line X18A at National Synchrotron Light Source (NSLS) at Brookhaven National Laboratory using a wide-angle position sensitive detector (PSD). The wavelength used was 0.9999 Å. The 2θ angles of all the XRD spectra presented in this article have been recalculated and converted to corresponding angles for λ = 1.54 Å, which is the wavelength of conventional X-ray tube source with Cu K_α radiation.

3 Results and discussion

3.1 Conductivity of the electrolyte

At room temperature the OEGDME500, 1 M LiPF₆ electrolyte has a conductivity of 0.48×10^{-3} S cm⁻¹ at 25 °C, which is lower than conventional lithium-ion battery electrolytes, but it is still in a technically attractive range. The conductivity has a rather strong temperature dependency as

Table 1 Ionic conductivity (S cm^{-1}) of OEGDME500, 1 M LiPF₆ as a function of temperature

Temp. (°C)	25	45	65	85
Conductivity (S cm^{-1})	0.48×10^{-3}	1.20×10^{-3}	2.23×10^{-3}	3.78×10^{-3}

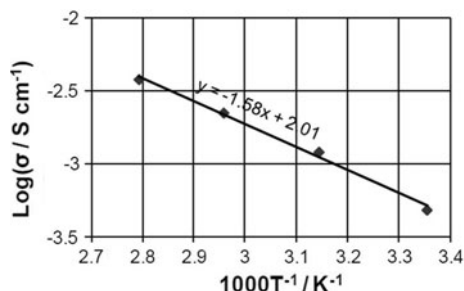
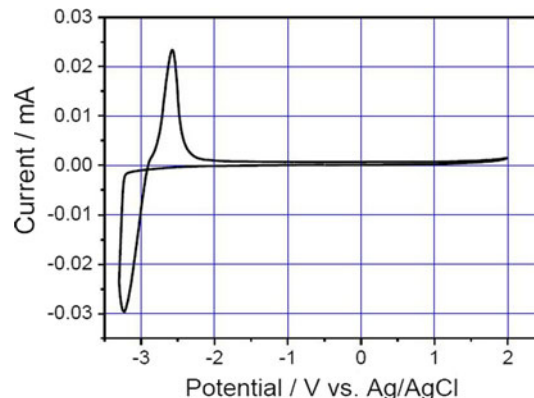
shown in Table 1. At 85 °C the conductivity is ten times higher ($3.78 \times 10^{-3} \text{ S cm}^{-1}$) than at 22 °C. OEGDME500 allows operating temperature above 100 °C with very attractive conductivities. Figure 1 shows the data listed in Table 1 as an Arrhenius plot. From the slope, we evaluate 30.7 kJ mol⁻¹ as the apparent activation barriers for ionic transport.

3.2 Electrochemical stability of the electrolyte

The window of electrochemical stability of OEGDME500, 1 M LiPF₆ was tested using cyclic voltammetry with a 2.5-mm aluminum disc electrode at slow scan rate (0.5 mV s⁻¹). Figure 2 reveals that the electrolyte has a window of at least 5.3 V, where in the potential region -3.3 to 2.5 V versus Ag/AgCl lithium was reversibly reduced and oxidized and at +2 V versus Ag/AgCl only a minor anodic current could be observed.

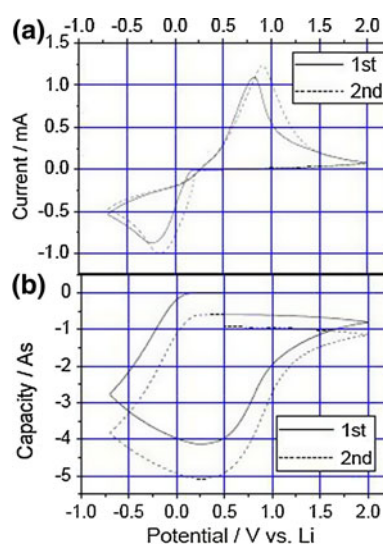
3.3 Lithium deposition and dissolution at Al electrodes

The electrochemistry of lithium at Al electrodes was investigated with a small Al electrode (0.05 cm²) and a larger Al electrode (2.8-cm² Al foil) in two different electrochemical cell arrangements. The small electrode was tested in a three-electrode cell typically used in voltammetric studies, where the Al electrode, the counter electrode and reference electrode was exposed as disc electrodes to the electrolyte. The disc electrodes were arranged alongside at the bar electrode. The results of this investigation are presented in Fig. 2. It shows that the deposition of the lithium started only at an over potential of about 250 mV at the scan toward negative potentials. However, during the back scan the current curve is crossing the zero current line at a potential close to the Li/Li⁺

**Fig. 1** Arrhenius plot of OEGDME500, 1 M LiPF₆. (data as listed in Table 1)**Fig. 2** Cyclic voltammogram of an Al electrode (0.05 cm²) in OEGDME500, 1 M LiPF₆. Reference electrode: non-aqueous Ag/AgCl. Counter electrode: Pt 0.05 cm². Scan rate: 0.5 mV s⁻¹

potential (2.95 V versus Ag/AgCl). Obviously, at that moment the aluminum electrode is acting like a lithium electrode, which means that at this scan rate (0.5 mV s⁻¹) not all of the lithium deposited during the cathodic scan was alloyed when the scan reached zero current at the reverse scan, thus the electrode was covered with a layer of lithium.

The results of the larger Al electrode are presented in Fig. 3. In this cell, a lithium foil was used as a counter electrode and in the same time as a reference electrode.

**Fig. 3** **a** First two current potential cycles of an Al electrode (2.8 cm²) in OEGDME500, 1 M LiPF₆. **b** Capacity change due to lithium reduction and re-oxidation during cycling. Scan rate: 0.2 mV s⁻¹

Unlike the alongside arrangement of the discs at the bar electrode, here the Al foil electrode is opposing the lithium foil electrode with an equal electrode surface. The working electrode (Al foil) was separated from the counter electrode (Li foil) by a filter paper, which was soaked in with electrolyte. Figure 3a shows the first two cycles of a voltammogram in the potential range between −0.7 and 2.0 V, versus Li/Li⁺. Due to the different cell arrangements and different scan rates the CV curves of the cell with the Al foil was looking different from that of the small Al disc electrode shown in Fig. 2. Figure 3 shows a higher peak to peak separation. This is most probably due to higher internal resistance of this cell. The Li deposition–dissolution CV shown in Fig. 3 has a large cathodic peak around −0.22 V versus Li/Li⁺ and an anodic lithium dissolution peak at about 0.8 V versus Li/Li⁺. In the second cycle, the CV is shifted toward somewhat more positive potentials. The fact that the negative current starts at more positive potentials in the second scan is most likely due to surface modification of the Al electrode during the first cycle leading to a lower over potential for the lithiation process. The cathodic current starts in the first cycle at about +0.18 V versus Li/Li⁺ and at 0.26 V versus Li/Li⁺ at the second cycle. At the back scan (scan in the positive current direction) the zero current potential is 0.25 V versus Li/Li⁺ in the first and second cycle. This clearly indicates that during this slow scan (0.2 mV s^{−1}) in the range +0.26 V → −0.70 V → +0.26 V versus Li/Li⁺ all the deposited lithium is alloyed when the potential reaches the zero current potential again at +0.25 V versus Li/Li⁺. It is interesting that at a scan rate of 0.5 mV s^{−1} the zero current potential at the positive back scan corresponds to the Li/Li⁺ potential (Fig. 2) indicating a lithium depot at the surface, whereas at the scan rate of 0.2 mV s^{−1} (Fig. 3a) this seems not to be the case.

Figure 3b shows the integrated current curve of Fig. 3a, which is the capacity change due to lithiation and delithiation during the potential scans. It shows that the capacity is not completely going back to zero at the end of the first cycle. About 15% of the deposited and alloyed lithium could not be extracted from the Al electrode during the scan at anodic currents with a scan rate of 0.2 mV s^{−1}. This part of the alloyed lithium could not reach the surface of the electrode in time to be re-oxidized to Li⁺. The lithium reduction on the aluminum foil occurs at about 260 mV. From this “under potential” deposition of lithium, we estimate that the heat of formation of the Al–Li alloy ($\Delta G = -zF\Delta E$) should be $\geq -25.1 \text{ kJ mol}^{-1}$. We can only estimate a lower limit since we do not know if the alloying of Li with aluminum needs a certain activation energy, which would lower the observed “under potential.”

To confirm that aluminum is forming an alloy during cathodic scan we made an in situ XRD investigation during

a constant cathodic current flow (−0.2 mA) at a aluminum foil electrode (2.8 cm²). Figure 4 shows the measured Al electrode potential during this experiment. It also indicates the charge states, where in situ XRD's were measured. Figure 5 shows the measured X-ray diffraction pattern. They reveal the emerging of a new set of Bragg peaks, which were identified as Al₁–Li₁ alloy (JCPDS No. 71-0362). During the cathodic lithium alloying process the electrode potential decreased gradually but was still more positive than the Li/Li⁺ potential, even after 35 h, indicating that at this current density (0.071 mA cm^{−2}) the alloying process is faster than the lithium deposition process. If we assume that the diffusion coefficient of Li in the Al electrode would be in the order $10^{-10} \text{ cm}^2 \text{ s}^{-1}$, the time for Li to diffuse 25 μm (Al electrode thickness) would be 8.6 h ($t = d^2/2D$). Thus, the lithium source at the surface of the Al electrode could easily be distributed all over the electrode thickness during the 35 h of cathodic lithium production. Different data can be found in the literature concerning the diffusion coefficient of lithium in Al–Li electrodes. The diffusion coefficient depends also strongly on the concentration of lithium in the Al–Li alloy [15, 16].

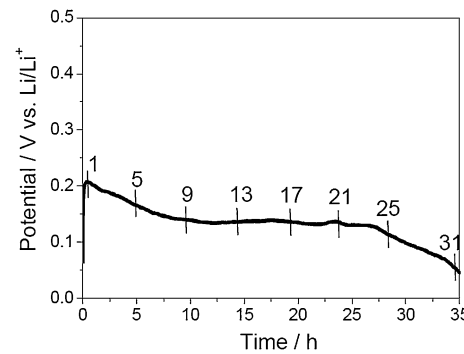


Fig. 4 Potential time curve of an Al electrode during electrochemical lithiation of an aluminum electrode (2.8 cm²) current: −0.2 mA. The numbers indicate the time in hours when the in situ XRD patterns (Fig. 5) were collected

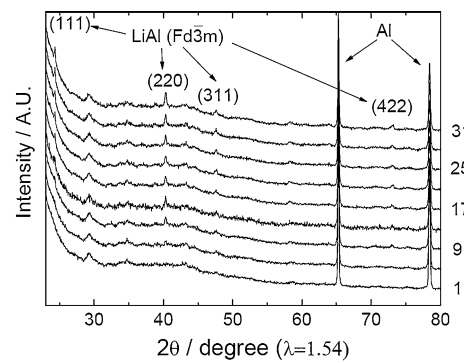


Fig. 5 In situ XRD measurements of a 2.8 cm² Al electrode during electrochemical lithiation revealing Al–Li alloy formation

Kumagai et al. revealed from potentiostatic measurements $10^{-10} \text{ cm}^2 \text{ s}^{-1}$ [17]. Values close to $7 \times 10^{-9} \text{ cm}^2 \text{ s}^{-1}$ were obtained by Jow et al. [18], Baranski et al. $7.7 \times 10^{-8} \text{ cm}^2 \text{ s}^{-1}$ [19], and Willhite et al. [20] obtained with NMR technique $8 \times 10^{-8} \text{ cm}^2 \text{ s}^{-1}$.

During the 35 h about $0.93 \times 10^{-4} \text{ mol}$ lithium are alloyed in 1 cm^{-2} of the Al foil, which itself contains $2.5 \times 10^{-4} \text{ mol cm}^{-2}$ aluminum. Thus, the stoichiometry would be close to Al_3Li_1 , a well known Al–Li alloy. From the XRD data, however, we conclude that most of the lithium forms an Al_1Li_1 alloy. The reflections of other possible alloys were not strong enough to be detected properly.

4 Conclusions

The OEGDME500, 1 M LiPF₆ electrolyte shows excellent electrochemical stability at low electrode potentials, which is impressively demonstrated with the electrochemical experiments illustrated in Figs. 2 and 3a. Figure 2 shows also negligible currents at very positive potentials. Thus, the OEGDME500, 1 M LiPF₆ electrolyte is very stable over a large potential range (about 5.5 V). Comparing with the conventional carbonate-based electrolyte, this electrolyte has a much higher boiling point, which is an important safety aspect. The conductivity at 25 °C of $0.48 \times 10^{-3} \text{ S cm}^{-1}$ may be on the lower limit for room temperature applications in lithium batteries. The high boiling point of this electrolyte, however, allows working at higher temperature where the conductivity is very attractive.

The electrochemical investigation of aluminum electrodes in this electrolyte reveals that aluminum is lithiated by an exergonic Al–Li alloy formation reaction. In situ XRD measurements proofed the Al_1Li_1 alloy formation during electrochemical deposition of lithium on aluminum electrodes. The electrode potential during the XRD experiment (35 h with a current density of 0.071 mA cm^{-2}) reveals that all the deposited lithium was immediately alloyed leaving no metallic lithium at the surface. The electrolyte solution could be stored over several weeks in vacuum or under Ar. However, after about 3 weeks a bluish

color developed, indicating some sort of charge transfer complex formation. This seems to be an inherent problem of LiPF₆. For long-term applications, it may be advantageous to use other electrolyte salts.

Acknowledgments This work was supported by the Assistant Secretary for Energy Efficiency and Renewable Energy, Office of Vehicle Technologies, under the program of “Hybrid and Electric Systems,” of the U.S. Department of Energy under Contract Number DEAC02-98CH10886. We would also like to thank the China Scholarship Council for the financial support of Y. N. Zhou.

References

1. Hong JS, Maleki H, Hallaj S, Redey L, Selman JR (1998) *J Electrochem Soc* 145:1489
2. Tobishima S, Yamaki J (1999) *J Power Sources* 81–82:882
3. Kaneko F, Masuda Y, Nakayama M, Wakihara M (2007) *Electrochim Acta* 53:549
4. Oh KW, Choi JH, Kim SH (2007) *J Appl Polym Sci* 103:2402
5. Marcinek M, Zalewska A, Zukowska G, Wieczorek W (2000) *Solid State Ionics* 136–137:1175
6. Kato Y, Ishihara T, Uchimoto Y, Wakihara M (2004) *J Phys Chem B* 108(15):4794
7. Tarascon JM, Armand M (2001) *Nature* 414:359
8. McBreen J, Lee HS, Yang XQ, Sun X (1999) In: 196th Meeting of the electrochemical society, October 17–22, Honolulu, HI
9. Elmer AM, Wesslen B, Sommer-Larsen P, West K, Hassander H, Jannasch P (2003) *J Mater Chem* 13:2168
10. Noto VD, Longo D, Müinchow V (1999) *J Phys Chem B* 103(14):2636
11. Wang XJ, Zhou YN, Lee HS, Nam KW, Yang XQ, Haas O (2010) *J Appl Electrochem*. doi:[10.1007/s10800-010-0231-6](https://doi.org/10.1007/s10800-010-0231-6)
12. Suresh P, Shukla AK, Shivashankar SA, Munichandraiah N (2004) *J Power Sources* 132:166
13. Yoon WS, Chung KY, McBreen J, Fischer DA, Yang XQ (2007) *J Power Sources* 174:1015
14. Balasubramanian M, Sun X, Yang XQ, McBreen J (2001) *J Power Sources* 92:1
15. Kishio K, Britain JO (1979) *J Phys Chem Solids* 40:933
16. Lantelme F, Iwadate Y, Shi Y, Chemla M (1985) *J Electrochem Soc* 187:229
17. Kumagai N, Kikuchi Y, Tanno K, Lantelme F, Chemla M (1992) *J Appl Electrochem* 22:728
18. Jow TR, Liang CC (1982) *J Electrochem Soc* 129:1429
19. Baranski AS, Fawcett WR (1982) *J Electrochem Soc* 129:901
20. Willhite JR, Karnezos N, Christea P, Brittain JO (1976) *J Phys Chem Solids* 37:1073